Journal of Catalysis 262 (2009) 169–176

Contents lists available at ScienceDirect

Journal of Catalysis

www.elsevier.com/locate/jcat

New insight on the nature of catalytically active gold sites: Quantitative CO chemisorption data and analysis of FTIR spectra of adsorbed CO and of isotopic mixtures

Anna Chiorino [a], Maela Manzoli [a], Federica Menegazzo [b], Michela Signoretto [b], Floriana Vindigni [a], Francesco Pinna [b], Flora Boccuzzi [a,*]

[a] Department of Inorganic, Physical and Materials Chemistry and NIS Centre of Excellence, Università di Torino, Via Pietro Giuria 7, 10125 Torino, Italy
[b] Department of Chemistry and Consortium INSTM, UdR Venezia, Università di Venezia, Dorsoduro 2137, 30123 Venezia, Italy

ARTICLE INFO

Article history:
Received 19 November 2008
Revised 19 December 2008
Accepted 22 December 2008
Available online 19 January 2009

Keywords:
Gold adsorbing sites
Adsorbed CO
FTIR
Quantitative chemisorption

ABSTRACT

FTIR absorption spectra of CO, of ^{12}CO–^{13}CO isotopic mixtures and of CO–$^{18}O_2$ interaction on gold catalysts supported on group IV oxides are reported together with CO quantitative chemisorption data. On Au/TiO_2 two kinds of metallic gold surface sites, mutually interacting, adsorb CO in spite of the low CO/Au ratio (0.03). On Au/ZrO_2, where a CO/Au ratio of 0.30 has been determined, mutually interacting corner sites on non-metallic gold nanoclusters are present. Finally, isolated and negatively charged gold nanoclusters have been evidenced on Au/CeO_2. Different absorption coefficients have been found. On all samples, by contacting CO–$^{18}O_2$ at 90 K, only $C^{16}O^{18}O$ is produced: gold sites are involved in the activation of both molecules. The largest amount of $C^{16}O^{18}O$ is produced on the CeO_2 supported sample, as a consequence of an easier activation of the oxygen on the anionic gold clusters and on the support.

1. Introduction

Gold catalysts are very active in the CO oxidation, in the PROX and in the WGS reaction. Therefore, they are good candidates for the catalytic production and purification of hydrogen for fuel cell applications [1]. Experimental and theoretical works suggest that for the PROX reaction the active sites for CO and oxygen activation may be uncoordinated sites of metallic gold nanoparticles [2]. Moreover, a role of cationic [3] and anionic [4] Au has been proposed and widely discussed in the last years. As for the WGS reaction, a very recent work on model samples [5] shows that water dissociates on oxygen vacancies of the oxide nanoparticles, in close contact with the gold sites. However, up to now key questions concerning the reaction mechanisms and the nature of the active sites are still without shared answers, possibly because the real catalysts have many of potential active centres, as stated very recently by Hutchings [6].

When studying real catalysts, it is useful to utilise different combined experimental methods, in order to distinguish and qualitatively determine the different gold sites exposed at the surface and also to find methods for quantitative estimation of these sites.

The analysis of the FTIR spectra after CO and CO isotopic mixtures adsorption at different temperatures on samples differently pretreated and of the FTIR spectra obtained after the CO interaction with $^{18}O_2$ can be very useful to get qualitative information on the nature and the structure of the gold active species in the CO oxidation. In addition, the relation between a defined amount of sites and the catalytic activity can be achieved by the analysis of CO quantitative adsorption volumetric measurements in specific experimental conditions, chosen on the basis of the spectroscopic experiments.

In 1978, Sheppard and Nguyen elegantly demonstrated the correlation that exists between the bonding geometry of adsorbed carbon monoxide on metals and the wavenumber of the C–O stretching vibrations [7]. They also drew attention to two other factors which can influence this wavenumber: the coexistence of surface atoms having different numbers of nearest neighbours and the dipolar interaction between adsorbed molecules. These factors are of particular importance in spectra from supported catalysts since coordinatively unsaturated edge and defect sites represent a large proportion of all the available adsorption sites on small particles. Dipolar interactions lead to coverage-dependent values of the wavenumber, since the predominant effect is to couple the vibrations of individual molecules to produce collective oscillations having infrared active modes at vibrational frequencies higher than the isolated singleton molecule. In subsequent years, these factors have been extensively studied on single crystal substrates. In particular, investigations using stepped surfaces have allowed more controlled studies on the influence exercised by the coordination

* Corresponding author. Fax: +39 011 6707855.
E-mail address: flora.boccuzzi@unito.it (F. Boccuzzi).

0021-9517/$ – see front matter
doi:10.1016/j.jcat.2008.12.017

Table 1
Properties of the examined samples.

Sample	Au (wt%)	BET surface area (m^2/g)	Au TEM size
Au/TiO_2	1.51	55	3.8 ± 0.8 nm
Au/ZrO_2	1.94	92	1.6 ± 0.6 nm
Au/CeO_2	3.0	118	Bimodal >10 nm and <1 nm

changing of the surface atom to which a CO molecule is bonded. It has been found that molecules at step sites do indeed exhibit different wave numbers from those on terrace sites, but the direction of the shift depends on the nature of the substrate. For example, on copper surfaces, step sites give rise to bands $\approx$15 cm^{-1} higher than terrace sites do [8], while on platinum the step site bands are shifted by a similar amount, but in the opposite side [9]. This difference has been rationalised in terms of the relative balance of σ and π bonding of the two surfaces: on both metals, bonding at step sites is stronger than at terrace ones, but on platinum the increased bonding interaction is associated with increased back-donation of metal electrons into the molecule's $2\pi^*$ orbital, and hence with a fall in wavenumber, whereas on copper and gold it is believed that the predominant change is a reduction in the occupancy of the σ orbital, with a concomitant shift to higher wavenumber [10]. It has also been found that the observation of bands due to molecules on the two types of site is complicated by the dipolar coupling interactions which tend to transfer intensity from low wavenumber bands to their higher wavenumber counterparts. As a consequence, the FTIR intensities of CO absorption bands are useful for a qualitative determination of the nature of the adsorbing active sites. In a number of cases, isotopic mixtures can be used to modify these interactions in order to clarify the vibrational spectra. Up to now such kind of data have been discussed for small gold particles [11], but were not yet available for small supported clusters nor for cationic and anionic species. Here we will present these data. Moreover, independent volumetric quantitative data of the gold adsorbing sites on some different catalysts will be presented, in order to compare more deeply different catalysts.

The absorption changes, both in position and shape, observed with the temperature and with the isotopic mixtures composition will be examined and interpreted. The assignments to the adsorption on corner, edge, borderline or cluster sites in gold nanostructured catalysts will be discussed, looking at the related quantitative chemisorption data.

2. Experimental

2.1. Materials

The examined catalysts, reported in Table 1, were all prepared by the deposition–precipitation method (dp). The Au/TiO_2 sample is an Au/TiO_2 reference catalysts provided by the World Gold Council [12]. As for the Au/ZrO_2 sample, the support was prepared by precipitation from $ZrOCl_2 8H_2O$ (Fluka) at constant pH (pH = 8.6), aged under reflux conditions for 20 h, washed free from chloride ($AgNO_3$ test) and dried at 383 K overnight. Then, the support was heated up to 923 K in flowing air for 6 h, followed by cooling to room temperature (hereafter denoted as r.t.) [13]. Gold was deposited on the calcined support maintaining constant pH = 8.6 throughout the preparation using a NaOH aqueous solution (0.5 M) (Riedel–de Haen). After filtration, the catalysts were finally dried at 310 K for 15 h. The Au/CeO_2 sample was prepared, as reported in [14], by deposition–precipitation of gold hydroxide on ceria suspended in water by the ultrasound technique.

2.2. Methods

FTIR spectra were taken on a Perkin–Elmer 1760 spectrometer (equipped with a MCT detector) with the samples in self-supporting pellets introduced in a cell allowing thermal treatments in controlled atmospheres and spectrum scanning at controlled temperatures (from 120 K to r.t.). From each spectrum, the background before the inlet of CO was subtracted. Band integration was carried out by "Curvefit," in Spectra Calc (Galactic Industries Co.). The obtained integrated areas were normalised to the Au content of each sample.

CO pulse chemisorption measurements were performed at 157 K. An inexpensive home made equipment was used for pulse chemisorption [15,16]. In principle the system was made of a U-shaped Pyrex reactor equipped with an oven controlled by a PID temperature programmer, mass flowmeters, sampling valve, a Gow-Mac TCD detector and a quadrupole mass detector. Before chemisorption the following standard pretreatment procedure was applied: the sample (200 mg) was reduced in H_2 flow (40 ml min^{-1}) at 423 K for 30 min, cooled in H_2 to r.t., purged in He flow and finally hydrated at r.t. The hydration treatment was performed by contacting the sample with a He flow (10 ml min^{-1}) saturated with water (2.7 mmol(H_2O) m^{-2}). The sample was then cooled in He flow to the temperature chosen for CO chemisorption. The temperature of 157 K was attained by an ethanol–liquid nitrogen cryogenic mixture temperature in a Dewar flask, therefore no cryostatic equipment was required. The gas uptake was measured from a sequence of small pulses until saturation was obtained. The following operating conditions were used: pulse size (0.4 ml), CO content in pulses (5 vol%), helium flow rate (30 ml min^{-1}), time interval between pulses (4 min).

3. Results and discussion

3.1. Spectroscopic data and quantitative chemisorptions of CO adsorbed on gold supported on titania, zirconia and ceria

In Fig. 1 the spectra of CO adsorbed on gold supported on the titania, zirconia and ceria, after reduction at 423 K, hydration at r.t. and successive cooling down to 120 K are shown (fine curves) together with the CO spectra recorded after heating up to 157 K. To our experience [15], this pretreatment is the most suitable one for a comparison of different gold catalysts on different supports, since the mild reduction eliminates the oxygen bonded to the surface of very small gold particles [17], while the hydration saturates the support cation sites at 157 K, preventing CO chemisorption at this temperature (see bold curves).

Big differences in shape, maximum position and intensity of the bands are evident in the 2100–2060 cm^{-1} frequency range. As for Au/TiO_2 (Fig. 1a), in addition to the quite strong and narrow band at 2098 cm^{-1}, a shoulder at lower frequency is observed. Both absorptions are due to CO adsorbed on gold sites [18]. Moreover, two additional components, at 2175 and 2150 cm^{-1}, are also present (fine curve). The former band is ascribed to the interaction of CO with Ti^{4+} cationic sites and the latter one is assigned to the interaction with the surface OH groups. Both these bands are completely depleted by increasing the temperature up to 157 K, while the 2098 cm^{-1} one and the low frequency shoulder slightly decrease in intensity (bold curve).

Similar experiments at 120 K performed on Au/ZrO_2 and illustrated in Fig. 1b, show a very intense band centred at 2094 cm^{-1} and a weak component at 2150 cm^{-1}, the last one being depleted by heating up to 157 K. The position of the band at 2094 cm^{-1} is close to that observed on Au/TiO_2, however in this case the band is broader and more symmetric in shape [13].

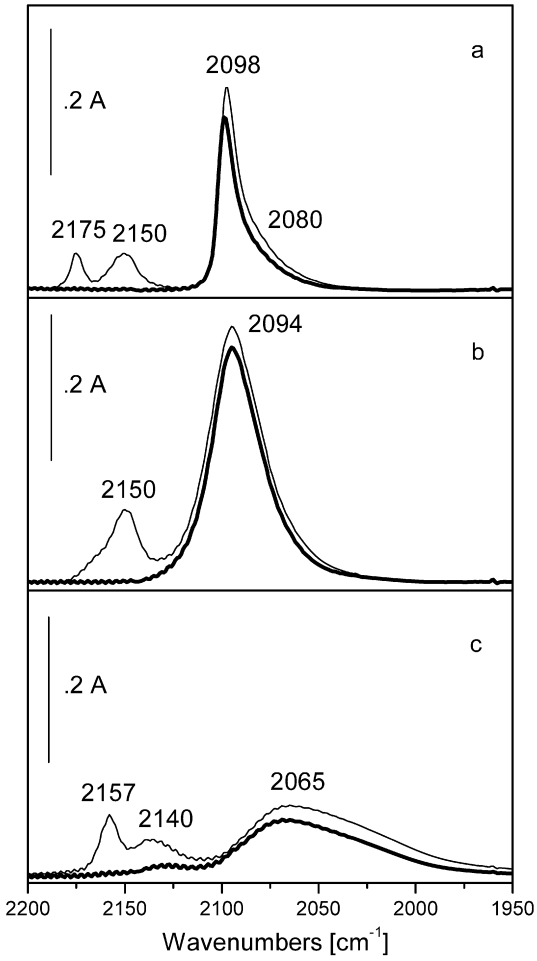

Fig. 1. FTIR spectra of CO adsorbed at 120 K (fine curves) and 157 K (bold curves) on gold supported on TiO_2 (a), ZrO_2 (b) and CeO_2 (c). The samples were reduced at 423 K, hydrated at r.t. and cooled down to 120 K before the CO inlet. All spectra have been normalised to the gold content of each pellet.

Table 2
Quantitative CO chemisorptions and FTIR integrated intensities at 157 K.

Sample	Au (wt%)	mol_{CO}/mol_{Au}	Integrated area (cm^{-1}/mol_{Au} ($\times 10^3$))	Absorption coefficient (cm^{-1} mol^{-1} ($\times 10^4$))
Au/TiO_2	1.51	0.033	1.05	3.2
Au/ZrO_2	1.94	0.301	5.41	1.8
Au/CeO_2	3.0	0.081	1.07	1.3

Fig. 1c shows the same experiment made on Au/CeO_2: a broad band, downshifted to 2065 cm^{-1} is evident, with two additional components at 2157 and 2140 cm^{-1}. The former is due to the interaction of CO with Ce^{4+} sites and the latter is ascribed to CO on Ce^{3+} sites and/or surface OH groups. Moreover, these bands are almost completely depleted by heating up to 157 K. The band at 2065 cm^{-1} is assigned to CO adsorbed on negatively charged gold nanoclusters, as already discussed in previous papers [19,20]. Therefore, on the basis of these preliminary spectroscopic experiments, quantitative volumetric measurements (Table 2) made at 157 K can be taken quite confidently as related exclusively to the amount of CO adsorbed on gold sites [15].

In Table 2 the integrated intensities of the absorption bands related to gold, i.e. the bands in the 2100–2060 cm^{-1} range, in the spectra taken at 157 K are summarised. All bands have been normalised to the gold content and compared with the volumetric chemisorption data for CO on gold supported on the three supports, titania, zirconia and ceria.

The volumetric experiments show that the molar ratio between adsorbed CO and gold on Au/TiO_2 is quite low (3.3%), almost 10 times larger than on Au/ZrO_2. These data are in agreement with the HRTEM results, summarised in Table 1, that indicate very different mean particle size of the two samples. An intermediate value of the ratio (0.081) is obtained for gold supported on ceria (Table 2), that exhibits a bimodal gold size distribution, as reported in Table 1. It can be inferred that on this sample the adsorption occurs with an high CO/Au ratio only on the nanoclusters observed by HRTEM, since the big particles with size larger than 10 nm do not adsorb CO and lower the CO/Au ratio.

The ratio between the data reported in column 4 and those in column 3 (Table 2) gives the values of column 5, that are the absorption coefficients of CO adsorbed on the different gold sites of the three samples. We found some differences among the three catalysts. In particular, the absorption coefficient of CO adsorbed on the gold particles supported on titania is higher than the absorption coefficients of CO adsorbed on gold sites on zirconia and ceria. This feature may be correlated to a changing of the nature of the adsorbing sites, i.e. to the transition from the metallic nature of gold on titania to the non-metallic one of gold nanoclusters supported on zirconia and ceria.

The absorption coefficients of CO adsorbed on these clusters are quite similar, but that of CO on gold supported on ceria is lower. In order to get a deeper understanding on these differences, isotopic mixture experiments at different equilibrium pressures and temperatures will be illustrated in the next section.

3.2. ^{12}CO and ^{12}CO–^{13}CO spectroscopic data on Au/TiO_2, Au/ZrO_2 and Au/CeO_2

The IR absorption spectra on Au/TiO_2 produced by adsorption of 15 mbar of CO at r.t. and their evolution by decreasing the CO pressure are shown in Fig. 2a. The sample has been calcined previously at 673 K and reduced at 423 K.

The maximum of the band (2110 cm^{-1}) is blue-shifted in respect to that reported in Fig. 1a (bold curve), as a consequence of the higher temperature and, therefore, of the lower coverage. The maximum of the absorption gradually blue shifts from 2110 cm^{-1} up to 2117 cm^{-1} by reducing the equilibrium pressure and its integrated intensity smoothly decreases. However, the shape and the asymmetry from the low frequency side remain still present in all spectra.

The shift is the result of lateral interactions that can be due to two different phenomena, a static or chemical effect and a dynamic or vibrational effect. The former can produce shifts in both directions, while the latter produces always a shift towards high wavenumbers. Experiments with isotopic mixtures allow the separation of these two components. Fig. 2b shows the spectra produced by interaction of a ^{12}CO–^{13}CO (1:1) mixture at different equilibrium pressures with the Au/TiO_2 sample.

In the spectrum obtained by contacting the sample with 15 mbar of this mixture, bands at 2096 cm^{-1} and 2049 cm^{-1} are observed. The ^{12}CO component is red-shifted by −14 cm^{-1}. Moreover, the two bands, assigned to ^{12}CO and ^{13}CO molecules adsorbed on gold metallic sites, are significantly broader (FWHM 22 cm^{-1}) than the band at 2110 cm^{-1}, detected after interaction with pure ^{12}CO (FWHM 10 cm^{-1}) and reported in Fig. 2a. These features have been analysed by a curvefitting procedure. The curvefits of the spectra taken in 8 mbar of ^{12}CO and in 8 mbar of ^{12}CO–^{13}CO (1:1), made by the addition of two and four Lorentzian bands, respectively, are shown in the insets of Figs. 2a and 2b. Particularly, the high frequency component is much stronger than the low frequency one in the inset of Fig. 2a, while, in the inset of Fig. 2b, the two components of each band have a quite similar intensity.

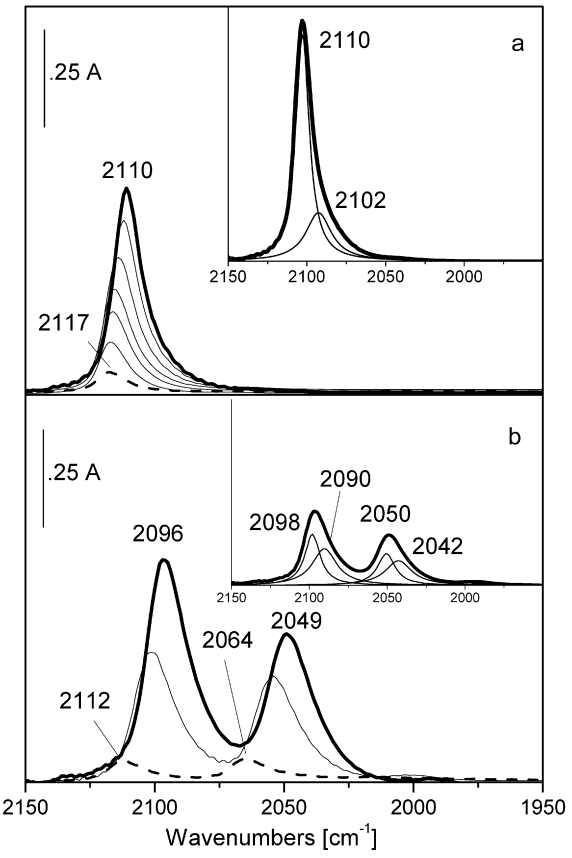

Fig. 2. IR absorption spectra produced by adsorption at r.t. of 15 mbar of ^{12}CO (a) and of ^{12}CO–^{13}CO (1:1) (b) and by decreasing pressure on Au/TiO_2 reduced at 423 K and hydrated at r.t. Insets: Curvefit of spectra taken in 8 mbar of ^{12}CO (a, bold line) and 8 mbar of ^{12}CO–^{13}CO (1:1) (b, bold line) on Au/TiO_2.

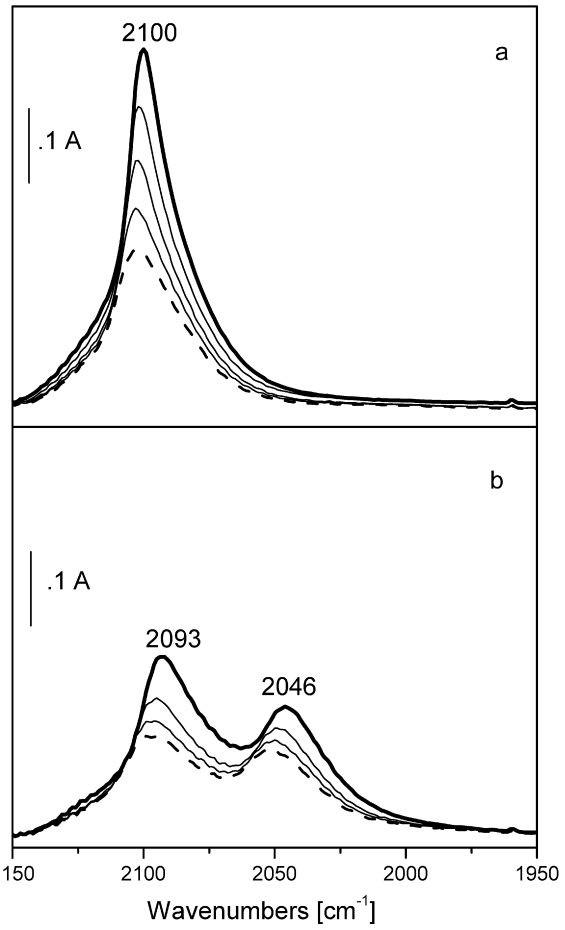

Fig. 3. IR absorption spectra produced by adsorption of 4 mbar of ^{12}CO (a) and of ^{12}CO–^{13}CO (1:1) (b) at increasing temperatures from 120 K up to r.t. on Au/ZrO_2 reduced at 423 K and hydrated at r.t.

The large difference in the intensity of the two components in pure ^{12}CO could be due either to an intrinsic very different amount of two kinds of non-interacting surface sites or to two strongly interacting sites. The broadening of the two bands in the isotopic mixture rules out the first hypothesis and indicates rather clearly that the two kinds of sites are mutually interacting. In fact, as shown in the inset of Fig. 2b, the two absorption bands, at 2096 cm^{-1} and at 2049 cm^{-1}, are made by the superposition of two components, of quite similar intensity. By reducing the equilibrium pressure the absorptions gradually reduce their intensities and shift towards high frequency up to 2112 and 2064 cm^{-1}.

A further remark is that the two bands display a significant intensity difference at the maximum coverage while they have almost the same intensity at low coverages: the relative intensity change with the coverage is another clear indication that the adsorption sites are mutually interacting and vibrationally coupled. The readmission of pure ^{12}CO after outgassing of the mixture produces an absorption spectrum with the same line-width, shape and intensity of those shown in Fig. 2a. Therefore, the higher line-width observed when contacting the mixture instead of the pure ^{12}CO can be explained only by a lower degree of coupling between the oscillators. These data are a clear evidence that two kinds of adsorbing site, mutually interacting, are present on gold particles supported on titania. An intensity transfer from the low frequency band to the high frequency one occurs at high coverages and in pure ^{12}CO, while the coupling is reduced at lower coverages or in the isotopic mixtures. Moreover, these spectroscopic features quite clearly indicate a high homogeneity of exposed and uncoordinated gold sites. The behaviour is definitely different from the heterogeneous broadening usually observed on many dispersed metals, characterised by structural and chemical heterogeneity in the adsorption sites, not coupled vibrationally. In that case, no shifts are observed by decreasing the coverage.

Figs. 3a and 3b show the spectra run at increasing temperatures, starting from 120 K, in the presence of a constant amount of gas, after adsorption on Au/ZrO_2 of ^{12}CO and ^{12}CO–^{13}CO (1:1), respectively. The sample has been previously reduced at 423 K. The increase of the temperature produces an effect similar to the reduction of the equilibrium pressure, i.e. a decrease of the surface coverage. In Fig. 3a, a band centred at 2100 cm^{-1} is shown, its position being similar to that observed on the Au/TiO_2 sample at the maximum coverage. However, in this case the maximum shows only minor shifts by decreasing the coverage, i.e. by increasing the temperature. Moreover, the interaction with the ^{12}CO:^{13}CO (1:1) mixture produces two bands at 2093 cm^{-1} and 2046 cm^{-1}, that are broader than the one in pure ^{12}CO (Fig. 3a) and that smoothly shift up by increasing the temperature. There are at least three indications that the adsorbed CO molecules are mutually interacting also on this sample:

(i) the shift of the ^{12}CO mode from 2100 cm^{-1} in pure ^{12}CO to 2093 cm^{-1} in the mixture (even if smaller, −7 cm^{-1}, than that observed on Au/TiO_2, because of the small size of the gold nanoclusters on zirconia, as shown in Table 1);
(ii) the intensity of the ^{12}CO band is anyway higher than that of the ^{13}CO one (2046 cm^{-1}) at the lowest temperatures; and
(iii) the intensity of the two modes becomes quite similar at the higher temperatures.

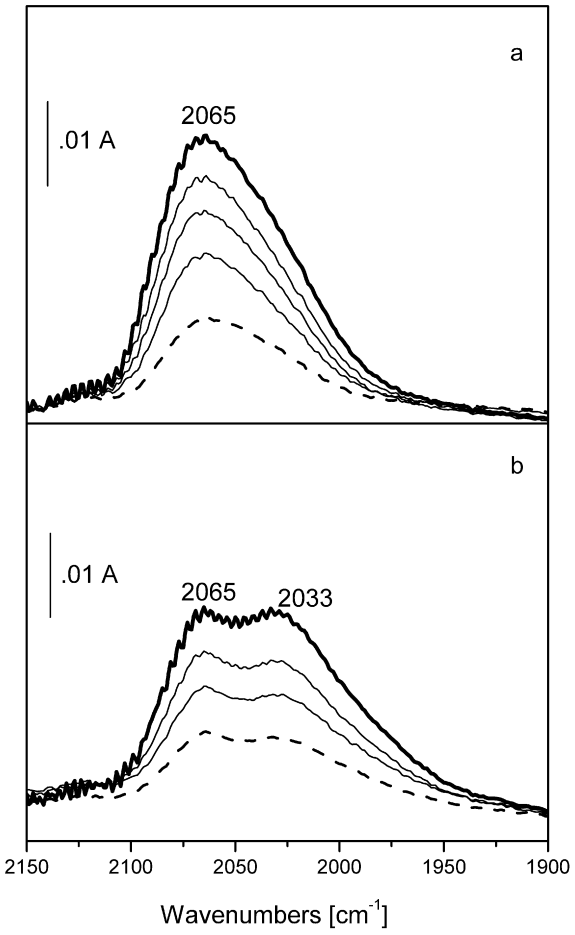

Fig. 4. IR absorption spectra produced by adsorption of 4 mbar of ^{12}CO (a) and of ^{12}CO–^{13}CO (b) at increasing temperatures from 120 K up to r.t. on Au/CeO_2 reduced at 423 K and hydrated at r.t.

Fig. 4 shows the behaviour of the absorption bands on Au/CeO_2 reduced at 423 K, in contact with 10 mbar of ^{12}CO (Fig. 4a) and with 10 mbar of ^{12}CO–^{13}CO (1:1) (Fig. 4b) at r.t. The shape, the position and the evolution of the bands by decreasing the gas phase pressure are remarkably different from those reported in the previously illustrated data, as for the Au/TiO_2 and the Au/ZrO_2 samples. At the maximum coverage, one band, significantly broader and red-shifted compared to that observed on the other two samples, is produced on Au/CeO_2. The red-shift at 2065 cm^{-1} can be taken as an indication that an electron transfer occurred from the reduced ceria to the gold nanoclusters, as previously discussed [19]. Two broad absorptions, at 2065 and 2033 cm^{-1} are produced by interaction with the isotopic mixture at the maximum coverage. By decreasing the pressure, the intensity of the bands decreases without significant changes in the position and in the relative intensity of the two components.

Looking at the different shape of the absorption, at the behaviour observed by decreasing the coverage and at the quantitative chemisorption data reported in Table 2, we get the indication that on Au/CeO_2 the adsorbing sites are isolated and not interacting differently from Au/TiO_2 and Au/ZrO_2.

3.3. Nature of the gold adsorbing sites on Au/TiO_2, Au/ZrO_2 and Au/CeO_2

We have shown by volumetric experiments that the molar ratio between adsorbed CO and gold sites on Au/TiO_2 is quite low, 3.3%. However, the FTIR experiments carried out at decreasing CO pressures and in the presence of the isotopic mixture evidenced that

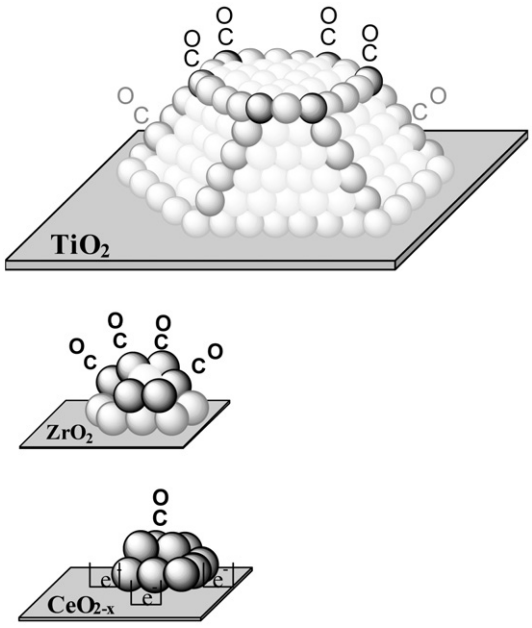

Scheme 1. Representation of gold species on the different supports.

two kinds of adsorbing sites, mutually interacting, are present on this catalyst. A representation of a gold particle with size (3.8 nm) and shape similar to those detected by TEM on titania is shown in Scheme 1.

It is widely accepted that CO adsorbs most strongly on surface uncoordinated defect sites, i.e. corners and edges, 6-fold and 7-fold coordinated, respectively. As this kind of particle contains a total estimated number of 410 gold atoms and 42 of them are located at corner and edge sites, a CO chemisorption ratio of 3.3% means 0.3 CO molecules per corner-edge Au, as we already proposed [15] on the basis of an even simpler assumption on a flat model-particle.

A possible arrangement of the adsorbed CO following the ratio calculated for the uncoordinated sites is proposed in Scheme 1, where all the corner 6-fold coordinated atoms and 1/3 of the lateral edge sites are covered by CO.

As for the adsorption sites of gold on zirconia, it has been shown that the spectroscopic features are quite similar. However, only one kind of adsorbing sites mutually interacting has been evidenced. We know from Table 2 that on Au/ZrO_2 the molar ratio CO/Au is about 10 times, while the integrated intensity is 5 times larger than that obtained for Au/TiO_2. The big ratio between CO and Au can be taken as an indication that a large fraction of the gold is uncoordinated and exposed at the surface, i.e. almost all Au atoms are in corner or interface positions (see Scheme 1). The interface atoms are more coordinated and therefore less able to coordinate CO, while all the corner sites can adsorb CO. We already pointed out that the variation of the absorption coefficient of CO adsorbed on Au sites observed when passing from zirconia to titania (Table 2) may be mainly correlated either to a changing of the nature of the adsorbing sites, i.e. to the transition from a metallic behaviour to a non-metallic one or to changes in the overcrowding and depolarisation effects. It is well known that on metallic surfaces the only modes which have significant infrared activity are those which own a variation of the dipole moment perpendicular to the metal surface. Physically, this is because the image dipole within the metal contributes to increase the intensity of the band. The image dipole contribution cannot be considered any more for the small gold nanoclusters of Au/ZrO_2, because the metallic character is lost. In the case of Au/CeO_2, as widely reported in Refs. [19,20], we cannot refer to the mean particle size to discuss the chemisorption stoichiometry, taking into account that this sample

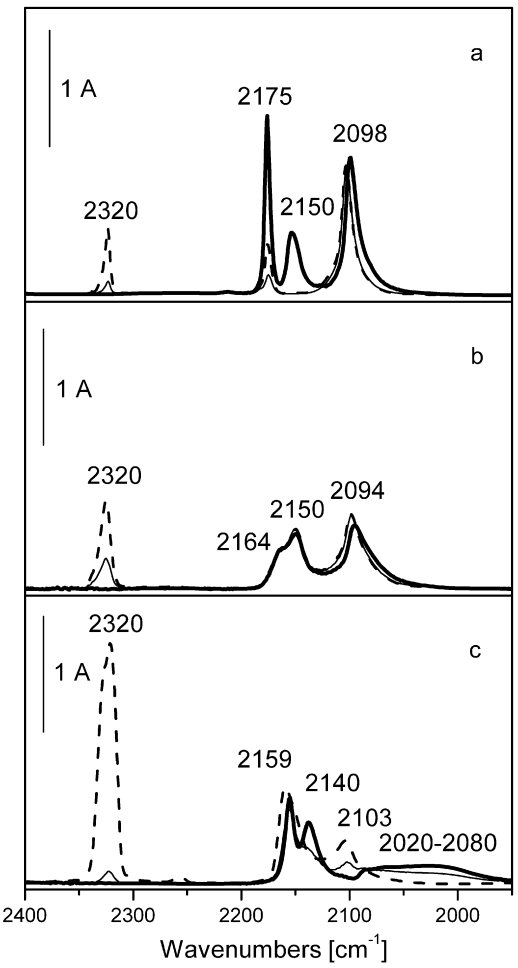

Fig. 5. Evolution of FTIR spectra at 120 K after the inlet of $^{18}O_2$ on preadsorbed CO on Au/TiO_2 (a), Au/ZrO_2 (b) and $AuCeO_2$ (c) reduced at 423 K (bold curve); after 2 and 10 min (fine and dashed curves).

exhibits both nanoclusters and quite large particles. The large CO chemisorbed volume must be mainly related to the presence of the Au nanoclusters where almost all of the atoms are exposed at the surface (see Scheme 1), whereas the large particles give no contribution to the chemisorption. In the previous section, we pointed out that the red-shift of the absorption maximum and the results of the isotopic mixture experiments suggest that the adsorbing sites are almost isolated, not interacting each other and negatively charged by an electron transfer from the reduced support. Also for this sample the absorption coefficient was found smaller than the one related to Au/TiO_2, in agreement with the non-metallic nature of the adsorbing sites (nanoclusters, as previously discussed for Au/ZrO_2).

3.4. FTIR spectra of CO–$^{18}O_2$ interactions at 90 K on Au/TiO_2, Au/ZrO_2 and Au/CeO_2

Fig. 5 shows the effect of $^{18}O_2$ contact at 90 K on the preadsorbed CO during the first 2–10 min on the three catalysts. Looking at the spectra reported in Fig. 5a, it appears evident that: (i) the low frequency component of the CO absorption band, due to CO on edge sites, is eroded as a consequence of reaction with coadsorbed $^{18}O_2$; (ii) the CO on the corner sites remain unperturbed; (iii) only one CO_2 species is produced, $C^{16}O^{18}O$. Quite similar features are also observed as for the interaction CO–$^{18}O_2$ at 90 K on Au/ZrO_2 (Fig. 5b). As for the Au/CeO_2 (Fig. 5c), some bigger differences are evident: the broad and weak band at 2020–2090 cm^{-1},

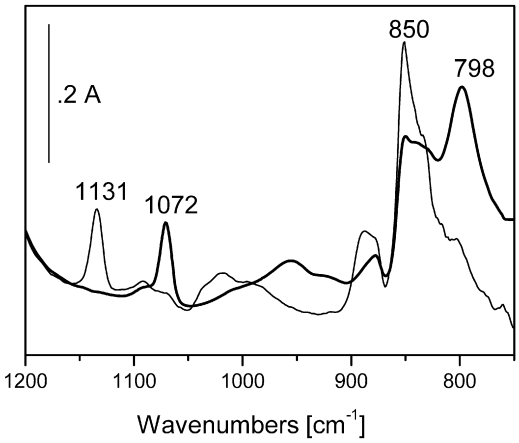

Fig. 6. FTIR spectra after the inlet of $^{16}O_2$ (fine curve) and $^{18}O_2$ (bold curve) at 120 K on CO preadsorbed on $AuCeO_2$ reduced at 423 K in the 1200–750 cm^{-1} range.

related to CO adsorbed on almost isolated and negatively charged gold sites is converted in a narrow and sharp one at 2102 cm^{-1}, i.e. is converted in the typical band of CO adsorbed on neutral gold corner sites. Moreover, the band at 2140 cm^{-1}, related to CO adsorbed on Ce^{3+} sites, is converted into CO on Ce^{4+}; anyway, also in this case only the $C^{16}O^{18}O$ is produced (band at 2324 cm^{-1}), in a larger amount than on the other two samples, (looking at the intensity of the $C^{16}O^{18}O$ absorption band).

Additional differences between Au/CeO_2 and the other two samples, Au/TiO_2 and Au/ZrO_2, are evident looking at the carbonate region and at the region where activated oxygen molecules can be detected. On Au/CeO_2, quite strong bands at 1640 and 1287 cm^{-1}, due to carbonate-like species on the support, grow up after interaction with $^{18}O_2$ or $^{16}O_2$ (not shown for sake of brevity). On the contrary, only very weak bands are present on Au/TiO_2 and Au/ZrO_2 in the carbonate like region. These bands, slightly shifted in respect to those observed by interaction with $^{16}O_2$, indicate that only on Au/CeO_2 the oxygen molecules activated on reduced support are able to produce carbonate species, already at 90 K. The presence of activated oxygen molecules adsorbed on reduced ceria sites is clearly testified by well defined bands, at 1072 and at 798 cm^{-1}, that grow up during the $^{18}O_2$ interaction (Fig. 6, bold curve). These bands are shifted in respect to those produced by $^{16}O_2$ at 1131 and at 850 cm^{-1} (fine curve). The bands at 1072 cm^{-1} and 798 cm^{-1} can be ascribed respectively to superoxo and peroxo species $^{18}O_2^-$ and $^{18}O_2^=$ adsorbed on reduced ceria in close contact with the gold clusters, while the bands at 1131 and at 850 cm^{-1} are assigned to superoxo and peroxo species $^{16}O_2^-$ and $^{16}O_2^=$. The residual bands at ≈850 cm^{-1} in the $^{18}O_2$ experiment and the not labelled bands in the 1050–900 cm^{-1} are related to the previously not shown carbonate species. Very similar frequencies of the stretching mode of these species has been observed by Raman [21] in the spectra of reduced ceria with hydrogen at 673 K after adsorption of $^{18}O_2$ and $^{16}O_2$ at 93 K. The reduction temperature in our experiments is significantly lower (423 K) and it can be postulated that the created oxygen vacancies are located close to the gold clusters (see Scheme 2). Nolan et al. [22] showed, by DFT calculations, that the gold can substitutes Ce atoms in the surface layer, leading to strong structural distortions. It has been shown that the formation of one oxygen vacancy near a gold doping atom is energetically "downhill," i.e. favoured. Moreover, the Au dopant weakens the bond of the surrounding oxygen atoms, facilitating CO oxidation. They have also shown that the doping with gold of the (110) ceria surface produces, by interaction with CO, a carbonate-like structure in which two oxygen atoms are abstracted, the doping with gold of the (100) ceria surface produces, after con-

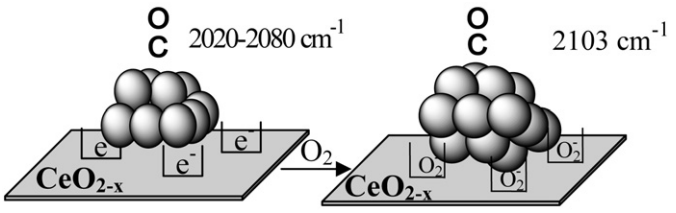

Scheme 2. Representation of the structure change of gold on reduced ceria after interaction with oxygen at 120 K.

tact with CO, molecular CO_2. Additionally, there is no absorption at 1131 cm^{-1}, where the superoxo species produced in the presence of $^{16}O_2$ absorb. This feature is a clear indication that, in the adopted experimental conditions, no exchange occurs between the oxygen atoms of the support and of the gas phase.

3.5. Nature of the active sites for CO and oxygen activation at low temperature

The so far illustrated results clearly show that there is no participation of oxygen atoms from the support to the reaction in the very mild conditions of our experiments. In all the cases here examined, only $C^{16}O^{18}O$ is produced by interaction with $^{18}O_2$, in spite of the structural and electronic differences between the surface gold species present on titania, zirconia and ceria, small metal particles, neutral small clusters and negatively charged clusters, respectively.

Different theoretical works ([23] and references therein) have shown that both involved molecules, CO and O_2, may be activated on two uncoordinated vicinal gold sites. On the small particles exposed on Au/TiO_2 the two vicinal sites may be two gold sites located on the edge of the particles, in fact the CO absorption band assigned to CO on edge sites is depleted by contact with oxygen. Similarly, the active sites of Au/ZrO_2 may be highly uncoordinated and mutually interacting gold sites, previously discussed, where both reactants molecules may be activated. An Au-only CO oxidation pathway has been suggested by Chen and Goodman [24] for ultrathin Au films on highly reduced titania. The authors evidenced an exceptionally high catalytic activity for carbon monoxide oxidation on these structures even if the support is not accessible to the reactants. Therefore, *independently from the size of the metal particles and/or nanoclusters on titania and zirconia, the reaction occurs by activation of the two reactant molecules on two vicinal uncoordinated gold sites*.

As for Au/CeO_2, the ^{12}CO–^{13}CO experiment previously illustrated showed that CO is adsorbed on isolated sites exposed on anionic and flat clusters, in close contact with oxygen vacancies and Ce^{3+}. After $^{18}O_2$ contact at 90 K the flat and negatively charged clusters are converted in more rounded clusters, exposing corner sites, as shown by the absorption band at 2103 cm^{-1}, and illustrated in Scheme 2. However, the oxygen atoms from the support do not take part in the CO oxidation reaction also in this case. The largest amount of $C^{16}O^{18}O$ produced on the ceria supported sample, may be a consequence of the participation to the reaction of $^{18}O_2$ activated on the oxygen vacancies close to the gold nanoclusters, without any exchange with the support oxygen atoms. It has been found by Nolan et al. [22] that the presence of a Au dopant lowers dramatically the energy for oxygen vacancy formation on all surfaces. The doping enhances the oxidative power of ceria: as, at catalytic temperatures, an oxygen vacancy near to the dopant is available, therefore the oxidation reactions will be facilitated by forming a second oxygen vacancy. An associative mechanism

$$^{18}O_2^* + CO^* \Leftrightarrow C^{16}O^{18}O + {}^{18}O^* + *$$

may be the dominant one in the low temperature conditions of our experiments. As discussed by Liu et al. [25] in a theoretical work on the catalytic role of gold in Au-based catalysts, CO oxidation can occur on Au step sites, where a metastable four centre O–O–CO intermediate state has been found. After formation of CO_2 the adsorbed oxygen may be easily removed by another CO. On the small particles exposed on Au/TiO_2 and on the Au/ZrO_2, these reactions can occur on two vicinal gold sites located on the edge and on the corner of the small metallic particles or on the clusters.

Similar findings in the oxygen molecule activation were reported for size-selected gold clusters, Au_n (where $n \leqslant 20$) supported on defect-rich MgO (100) films [26]. The high activity of this catalyst in the low temperature production of $C^{16}O^{18}O$ could be also due to an enhanced stabilisation of the oxygen molecule on the anionic gold nanoclusters [27], however there are no experimental evidences concerning this last hypothesis.

4. Conclusions

The combined analysis of ^{12}CO and ^{12}CO–^{13}CO FTIR absorption spectra and of quantitative chemisorption data allowed a deeper understanding of the relationship between the nanostructure and the physical and chemical properties of gold catalysts supported on the group IV oxides. The main points are:

(i) two kinds of mutually interacting sites (corners and edges) are the CO adsorbing sites on the gold metallic particles (mean size 3.8 nm) supported on titania. In spite of the low CO/Au ratio (0.03) the absorption coefficient is high;
(ii) corner sites, mutually interacting, exposed at the surface of non-metallic nanoclusters are the adsorbing Au sites on the zirconia supported sample, where a CO/Au ratio of 0.30 has been determined. The absorption coefficient is low, as a consequence of the non-metallic nature of the absorption sites and of the consequent lack of the image dipole contribution;
(iii) almost isolated and negatively charged are the gold adsorbing sites exposed on the ceria supported sample;
(iv) the CO–$^{18}O_2$ interaction at 90 K produces only $C^{16}O^{18}O$ on all samples, indicating that both molecules are activated on the gold sites; the largest amount of $C^{16}O^{18}O$ is produced on the ceria supported sample, as a consequence of the oxygen activation on the oxygen vacancies close to the gold nanoclusters.

Acknowledgments

The authors gratefully acknowledge the MIUR for financial support (COFIN 2006033400_002).

References

[1] G.J. Hutchings, M. Brust, H. Schmidbaur, Chem. Soc. Rev. 37 (2008) 1759–1765.
[2] D.W. Goodman, Catal. Lett. 99 (2005) 1–4.
[3] Q. Fu, H. Saltsburg, M. Flytzani-Stephanopoulos, Science 301 (2003) 935–938.
[4] M.S. Chen, D.W. Goodman, Science 306 (2004) 252–255.
[5] J.A. Rodriguez, S. Ma, P. Liu, J. Hrbek, J. Evans, M. Perez, Science 318 (2007) 1757–1760.
[6] G.J. Hutchings, Dalton Trans. 41 (2008) 5523–5536.
[7] N. Sheppard, T.T. Nguyen, in: R.J.H. Clark, R.E. Hester (Eds.), Advances in Infrared and Raman Spectroscopy, Heyden, London, 1978, pp. 67–148.
[8] P. Hollins, K.J. Davies, J. Pritchard, Surf. Sci. 138 (1984) 75–83.
[9] B.E. Hayden, K. Kretzschmar, A.M. Bradshaw, R.G. Greenler, Surf. Sci. 149 (1985) 394–406.
[10] P. Hollins, Surf. Sci. Rep. 16 (1992) 51–94.
[11] C. Ruggiero, P. Hollins, Surf. Sci. 583 (1997) 377–379.
[12] Samples number 17C, supplied by World Gold Council, http://www.gold.org.
[13] F. Menegazzo, F. Pinna, M. Signoretto, V. Trevisan, F. Boccuzzi, A. Chiorino, M. Manzoli, Chem. Sus. Chem. 1 (2008) 320–326.
[14] D. Andreeva, V. Idakiev, T. Tabakova, L. Ilieva, P. Falaras, A. Bourlinos, A. Travlos, Catal. Today 72 (2002) 51.

[15] F. Menegazzo, M. Manzoli, A. Chiorino, F. Boccuzzi, T. Tabakova, M. Signoretto, F. Pinna, N. Pernicone, J. Catal. 237 (2006) 431–434.
[16] F. Menegazzo, F. Pinna, M. Signoretto, V. Trevisan, F. Boccuzzi, A. Chiorino, M. Manzoli, Appl. Catal. A, doi:10.1016/j.apcata.2008.12.004.
[17] V.A. Bondzie, S.C. Parker, C.T. Campbell, Catal. Lett. 63 (1999) 143–151.
[18] F. Boccuzzi, A. Chiorino, M. Manzoli, P. Lu, T. Akita, S. Ichikawa, M. Haruta, J. Catal. 202 (2001) 256–267.
[19] T. Tabakova, F. Boccuzzi, M. Manzoli, D. Andreeva, Appl. Catal. A Gen. 252 (2003) 385–397.
[20] G. Avgouropoulos, M. Manzoli, F. Boccuzzi, T. Tabakova, J. Papavasiliou, T. Ioannides, V. Idakiev, J. Catal. 256 (2008) 237–247.
[21] V.V. Pushkarev, V.I. Kovalchuk, J.L. D'Itri, J. Phys. Chem. B 108 (2004) 5341–5348.
[22] M. Nolan, V.S. Verdugo, H. Metiu, Surf. Sci. 602 (2008) 2734–2742.
[23] L.M. Molina, B. Hummer, Appl. Catal. A 291 (2005) 21–31.
[24] M. Chen, D.W. Goodman, Acc. Chem. Res. 39 (2006) 739–746.
[25] Z.-P. Liu, P. Hu, A. Alavi, J. Am. Chem. Soc. 124 (2002) 14770–14779.
[26] D. Stolcic, M. Fischer, G. Ganteför, Y.D. Kim, Q. Sun, P. Jena, J. Am. Chem. Soc. 125 (2003) 2848–2849.
[27] A. Sanchez, S. Abbet, U. Heiz, W.-D. Schneider, H. Häkkinen, R.N. Barnett, U. Landman, J. Phys. Chem. A 103 (1999) 9573–9578.